CHARACTERIZATION OF STRAIN HARDENING THREE DIMENSIONAL CRACK-TIP STRESS FIELD

By:

MUHAMMAD NAIM BIN ZAKARIA

(Matrix no.: 141678)

Supervisor:

Dr. Norwahida binti Yusoff

July 2022

This dissertation is submitted to

Universiti Sains Malaysia

As partial fulfillment of the requirement to graduate with honors degree in

BACHELOR OF ENGINEERING (MECHANICAL ENGINEERING)

UNIVERSITI SAINS MALAYSIA

School of Mechanical Engineering

Engineering Campus

Universiti Sains Malaysia

DECLARATION

This work has not previously been accepted in substance for any degree and is not being concurrently submitted in candidature for any degree.

Signed   (MUHAMMAD NAIM BIN ZAKARIA)

Date: 24/7/2022

Statement 1: this journal is the result of my own investigation, except where otherwise stated. Other sources are acknowledged by giving explicit references. Bibliography/ reference are appended.

Signed   (MUHAMMAD NAIM BIN ZAKARIA)

Date: 24/7/2022

Statement 2: I hereby give consent for my journal, if accepted, to be available for photocopying and for interlibrary loan, and for the title and summary to be made available outside organisations.

Signed   (MUHAMMAD NAIM BIN ZAKARIA)

Date: 24/7/2022

ACKNOWLEDGEMENT

In the name of Allah, the Most Gracious and the Most Merciful

First of all. All praises to Almighty Allah for his blessing and for giving me strength to complete this research within the given time frame. A very special appreciation are given to my supervisor, Dr. Norwahida binti Yusoff for her guidance and continuous support which I believe the key of success of this research. Her style in explaining and solving the problem I believe has guide me on the right path to complete this research and the completion of this thesis.

A very special appreciation was given to my parents for their strong support although I facing good and hard time throughout this research. I would like to thanks my siblings, Muhammad Hafiz, Muhammad Amin and Rabiatul Adawiyah for always giving me motivation when I almost giving up with the research and guiding me to regain the passion to complete this research.

Lastly, a highest thanks was given to my fellow roommates, Muhammad Muzakkir and Muhammad Nafiz that inviting me to join them completing the thesis together in the Microscopic lab which guiding me to complete the thesis on time. My thanks goes to technician of Microscopic lab, Mr. Idzuan Said that give me approval to use some space of the lab when writing thesis.

TABLE OF CONTENTS

LIST OF TABLES

vi

LIST OF FIGURES

LIST OF SYMBOLS

σ_o Yield stress

P_o Load limit

ε_o Elastic strain limit

a   Crack length

B   Compact Tension specimen thickness

E   Young's modulus

J   J-intergral

n   Strain hardening exponent

T_z Plane strain parameter in J-T_z approach

W   Compact Tension specimen width

σ Uni-axial stress

ε Plain strain

LIST OF ABBREVIATIONS

x

CT	Compact Tension
DOF	Degree of Freedom
FEA	Finite Element Analysis
2D	Two Dimensional
3D	Three Dimensional

CHEMOMETRICS AND PATTERN RECOGNITION METHODS WITH APPLICATIONS TO ENVIRONMENTAL AND QUANTITATIVE STRUCTURE-ACTIVITY RELATIONSHIP STUDIES

ABSTRAK

Penilaian integriti struktur konvensional mampu memberikan anggaran kegagalan tetapi penilaian itu kebanyakannya adalah masalah dua dimensi yang terhad kepada penyelesaian dua dimensi. Kebanyakan masalah dalam dunia sebenar adalah berdasarkan masalah tiga dimensi. Walaupun terdapat penilaian dan penyelesaian di dalam bidang tiga dimensi, pencirian dalam masalah tiga dimensi masih tidak lengkap. Oleh itu, kajian ini memberi motivasi untuk menilai lebih lanjut kesan pengerasan terikan pada medan hujung retakan dan untuk menilai sifat kehilangan kekangan hujung retakan dalam masalah patah.

Medan retak tiga dimensi elastik-plastik tulen telah diperiksa menggunakan analisis elemen terhad (FEA) melalui spesimen tegangan padat (CT). Kesan pengerasan terikan diperhatikan kerana peningkatan dalam eksponen pengerasan terikan akan mengurangkan tegasan. Kekangan luar satah dalam spesimen CT diperhatikan hilang dari satah pertengahan ke permukaan bebas.

Oleh itu, boleh disimpulkan bahawa kekangan di luar satah hilang apabila bergerak ke arah permukaan bebas. Dengan itu, terdapat lebih banyak bidang untuk menjadi penyelidikan untuk mengurangkan konservatisme pendekatan dua dimensi.

CHEMOMETRICS AND PATTERN RECOGNITION METHODS

WITH APPLICATIONS TO ENVIRONMENTAL AND QUANTITATIVE

STRUCTURE-ACTIVITY RELATIONSHIP STUDIES

ABSTRACT

Conventional structural integrity assessments capable in providing an estimation of failures but the assessment are mainly two dimensional problem that limited to two dimensional solution. Most of the problem in real world are based on the three dimensional problem. Although there are assessment and solution to the three dimensional fields, the characterization in three dimensional problem is still lacking. the present research, therefore, motivated to further assess effect of strain hardening to crack-tip field and to assess the nature of crack-tip constraint loss in fracture problem.

Elastic perfectly-plastic three dimensional crack-tip field have been examined using Finite Element Analysis (FEA) through Compact Tension (CT) specimen. The effect of strain hardening were observes as the increases in the strain hardening exponent will decreases the stress. Out-of-plane constraint in CT specimen were observed lost from mid-plane to free surface.

Therefore, it can be conclude that the out-of-plane constraint is lost when moving towards free surface. This, There is more area to be research to reduce the conservatism of two dimensional approach.

CHAPTER 1

INTRODUCTION

1.1   Brief overview of the overall structure of the project

Fracture mechanic is an important sector in the engineering field. Fracture mechanic commonly applies on the engineering structure. Fracture mechanics is the field of mechanics that study the propagation of cracks in material. As the design of modern structure become more and more complex, the significance of fracture mechanics is increasing rapidly. Knowledge in fracture mechanics is important in engineering structure as fracture mechanics is able to predict the maximum crack in a structure that a material can withstand before it fails. One of the examples is when the liberty ship vessel broke completely in two while sailing between Siberia and Alaska. The investigation revealed that the failures were caused by the combination of three factor and one of the factor is the ship welding contained crack-like flaws. Knowledge about fracture mechanics allows researcher to assess the structural integrity in which called   structural   integrity   assessment.

Structural Integrity Assessment is way to assess a structure whether the structure will be able to withstand the service condition safely throughout its lifetime. Structural integrity assessment defines the significant of an existing crack on an structural component. Structural integrity is important component of all structural engineering project both in mechanical and civil engineering such as buildings, dams, machine, devices and complex systems. The current ways of the assessment usually is based on two dimensional model but in the real situation, the real problem is three dimensional. Although a lot of research have been made in order to propose the solution of quantifying the three dimensional model, but there is still more sector in the fracture

mechanics to be research. Most of the current proposed solution is limited only to the certain condition of the three dimensional model. An approach to characterize three dimensional model is $J-\Delta\sigma$. The research about this approach was done by (Karh Heng Leong, 2020). This approach has been shown to be capable of quantifying in-plane and out-plane constraint using parameter $J/z\sigma_0$ but usage of this parameter is still limited to the specific fracture condition and cannot be used for other conditions. Other than that, the development using plain strain parameter T_z that is proposed by (Wanlin, 1995) that is used to define three dimensionality crack tip was proved by (Yusoff & Yusof, 2017) that the proposed solution is only limited to use at the mid-plane of the crack tip. As we can see the overall solution in quantification three dimensional crack tip model is still not perfect. It also shown that there is still a lot of research needed to be conduct in order to conclude the solution of three dimensional model. The quantification of three dimensional model is still needed to be investigate more. The effect of strain hardening to the crack tip stress field will going to be investigate in this paper.

1.2 Objectives of research

a) To characterize three-dimensional crack-tip stress field in consideration of the strain hardening response

b) To recognize the pattern of out-of-plane constraint loss in 3D cracked bodies

1.3   Problem statement

The assessment of structural integrity is a very important consideration in the engineering fields but the current structural integrity assessment scheme is rely based on 2D model. Although currently there are 3D model that are being used, but the 3D model itself is using simplified or generalized model of perfectly-plastic. One of the example is J$-\Delta\sigma$ approach by (Karh Heng Leong, 2020). The approach has the ability to quantify the three dimensional model but the approach seems to be limited to only certain fracture condition. Other than that the plain strain parameter T_z that is proposed by (Wanlin, 1995) that is used to define three dimensionality crack tip was proved by (Yusoff & Yusof, 2017) that the proposed solution is only limited to use at the mid-plane of the crack tip. From all the development that have been made by the researcher, it is clearly that the characterization three dimensional crack tip still need to be research more. Although a lot of research have been made, the sole solution in three dimensional characterization still far to be conclude. This research is mainly focused in characterization the three dimensional crack tip but it is influenced by the strain hardening

1.4   Scope of the project
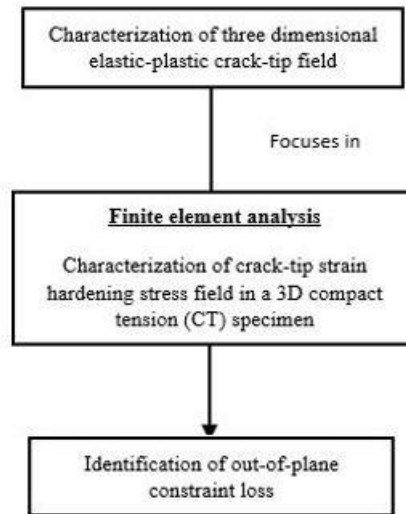
Figure 1.1   The overall scope of the research

The overall scope of the research work is diagrammatically outline in Figure 1.1. The final objectives for this research works is focusing in characterization of crack-tip strain hardening stress field. The result then investigate to determine the influence of out-of-plane constraint. For finite element analysis, a 3D compact tension specimen were develop using Abaqus software. the 3D compact tension specimen will undergo development process that include determination of material response, boundary condition, meshing and finally calculation of results, The 3D compact tension specimen examined through finite element analysis of three-dimensional full-field with sharp crack-tip. The research works then focused onto identification of out-of-plane constrain around the crack tip.

CHAPTER 2

LITERATURE REVIEW

2.1   2D Crack Tip Field

The theory of fracture mechanics started with two dimensional model when (Inglis, 1913) found the ideas and evidence for stress concentration effect. The idea then name as Inglis analysis where the analysis used in analysing an elliptical hole in a flat plate. The elliptical hole was assumed to be not influenced by the plate boundary. In his analysis, the dimension of the elliptical hole were 2a long and 2b wide. The graphical example of the elliptical hole on the plate was presented on the Figure 2.1
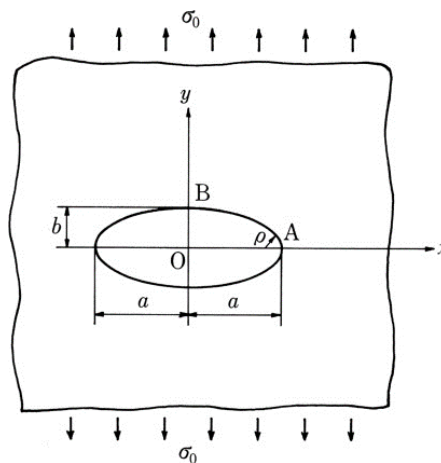
Figure 2.1   Elliptical hole in infinite plate

The stress at the major axis denoted by

$$\sigma_A = \sigma \left(1 + \frac{2a}{b}\right) = \sigma \left(1 + 2\sqrt{\frac{a}{\rho}}\right) \tag{2.1}$$

Where σ is the stress applied, a is the half crack length on major axis of the cracks, b is the half crack length on minor axis of the crack and $\rho = b^2/a$ is the radius of curvature at the end cracks on major axis. Inglis equation predict an infinite stress at the tip of sharp crack as ρ reaching zero which cause a lot of concern because of no material can sustain of infinite stress.

(Tian & Cui, 2005) have done a research to propose a solution in determining the crack-tip field and a solution for Model-I elastic-plastic crack-tip field in a bi-linear material. Other than that, this research was done to derive a formula for the critical value of J-integral in terms of T-stress for an elastic-plastic material. As for result, the present solution for elastic-plastic crack-tip field indicated that the elastic strain are depends on the value of T-stress as well as hardening exponents. In case of high hardening materials of n=3, the plastic strain curves are lower than elastic strain curves regardless the different T-stress value but for the low hardening material of n=9, plastic strain curves are lower compare to the elastic curves when the T-stress value is decrease. As the T-stress value decrease until certain point, the plastic curves then sharply increase.

The relation between J-integral and T-stress based in power-law hardening material was concluded by formula of:

$$\frac{J_c}{J_{Ic}} = f(\frac{T}{\sigma_o}, v, \varepsilon_o, \alpha, n)$$

(2.2)

The research concludes that the values of J_c for low hardening material was dependant on the value of T-stress but for high hardening material, it is the opposite. The research then concludes that the effect of T-stress in fracture mechanics is limited to the low hardening material.

2.1.1 J-integral

J-integral is a parameter that is developed by (Rice, 1968) in 1968. The parameter is focussed in characterization of crack-tip field of non-linear material. Other than that, the research are focussed in the determination of the stress around the hole on a plate. The elliptical hole are assumed to be a fine crack by making one axis to be very small. The equation expressed gives the rate of energy released per unit area of crack surface increase. The rate of energy release was evaluated as line integral along an arbitrary contour around the crack-tip. The direction of the arbitrary contour is in anti-clockwise as in Figure . The equation of J-integral was expressed as:

$$J = \oint w \ dy - \oint T . \frac{\partial u}{\partial x} dT \tag{2.3}$$

Where w is strain energy density and the second term is the work done by the external fore where T is the traction vector, and u is displacement vector. The arbitrary contour around the crack tip was demonstrated as Figure 2.2
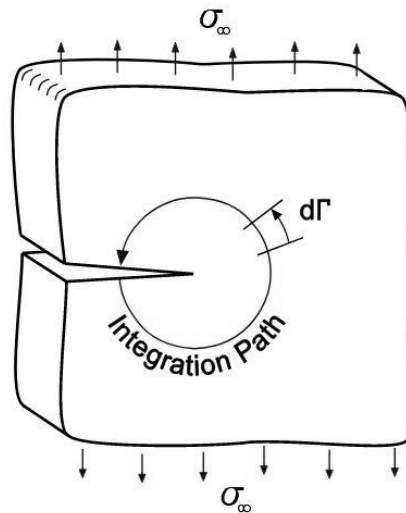
Figure 2.2   Arbitary field around the crack tip

This research work are mainly focussed on the effect of the strain hardening on the material, so in the next literature review, we will review the influence of strain hardening on the estimation of J-integral.

The research done by (Al-Abduljabbar, 2004) to observe the effect of strain hardening on the estimation of J-integral in CT specimen. The research was done by deriving new expression to visualise the strain hardening effect. In order to visualize the result, a parameter which is η and $\eta*$ factor where parameter of η -factor was used on non-hardening material and $\eta*$ used for hardened material. The parameter was used to visualize the result of hardened material and not hardened material. The value of η -factor and $\eta*$factor will determine the value of J-integral as the higher value of η -factor and $\eta*$factor causing the higher value of J-integral. The expression for η -factor and $\eta*$factor are as below:

$$\eta = 2\frac{1+\alpha}{1+\alpha^2} \tag{2.4}$$

$$\eta^* = 2\frac{(1+\beta)\Phi\alpha - (1+\beta)\alpha^2 - \beta\alpha^3}{[\Phi + (1+2\beta)\alpha^2](\Phi + \alpha^2)}2\alpha\Delta \tag{2.5}$$

Where α is crack length, β is strain hardening coefficient and Φ is equivalent to 1 in this research. Because of η -factor represent non-hardening material, the value of β in the equation is assumed to be $\beta = 0$.

The result for this research demonstrated in the Figure 2.3:
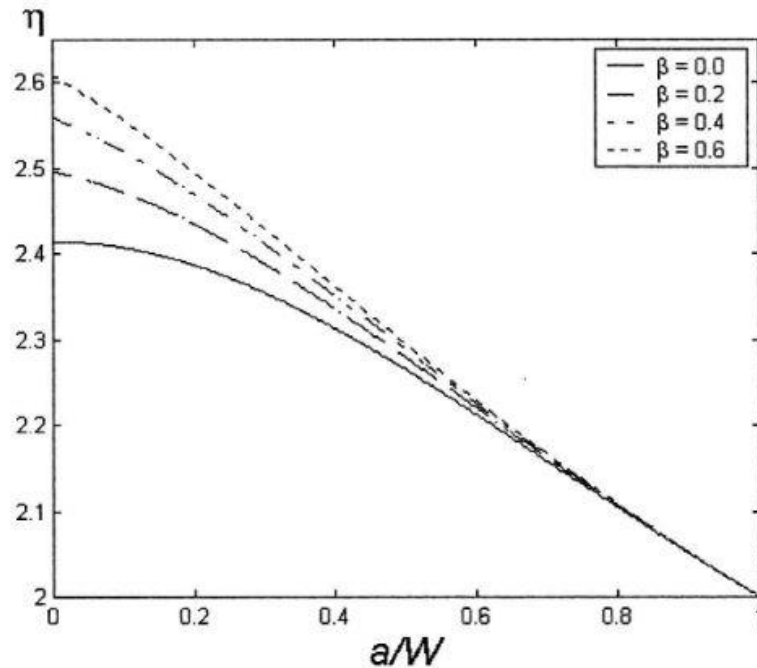
Figure 2.3 η-factor as a function of strain hardening coefficient, β

As for result, Figure 2.3 visualised the effect of strain hardening to the η-factor. In the result, $\beta = 0.0$ represent η- factor in which the result represent the non-hardening material while $\beta = 0.2, 0.4$ and 0.6 represent η^*-factor that represent hardened material. In the Figure 2.3, it is clearly that the exposure to strain hardening coefficient, β causing

9

in increasing the value of η^*-factor. The increasing of value of η^*-factor causing the higher value of J-integral.

2.1.2 Prandtl Slip Line

Prandtl slip line is an important crack-tip field for plain strain field where Prandtl slip line assumes that at the crack tip were surrounded with plastic region that forms a diamond shaped fields, the fields were separated into three different region there the region were name regions I, II and III. For both region I and III the area taken for this region is $\frac{\pi}{4}$ which is 45° and for region II is 90°. The region is as shown in Figure 2.4:
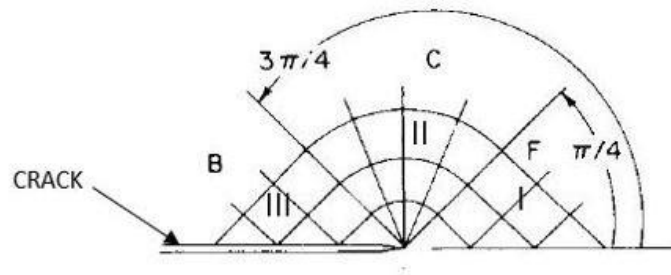
Figure 2.4 Prandtl slip line field

Prandtl slip line field are capable in describing the Mode-I plain strain stress field near a sharp crack tip. The relevance of Prandtl slip line were identified by (RICE, 1982). The slip line represents the maximum shear stress in which expressed in terms of yield stress in shear, k. Yield stress in shear, k were expressed in form:

$$\bar{\sigma} = \sigma_o = \sqrt{3}k$$

(2.6)

where $\bar{\sigma}$ is the equivalent stress.

The asymptotic stresses are calculated starting on the region I which is ahead of the crack tip. The expression are given by:

$$\sigma_{rr} = k(\pi + 1 - \cos 2\theta) \tag{2.7a}$$

$$\sigma_{\theta\theta} = k(\pi + 1 + \cos 2\theta) \tag{2.7b}$$

$$\sigma_{zz} = \sigma_m = k(1 + \pi) \tag{2.7c}$$

$$\sigma_{r\theta} = k \sin 2\theta \tag{2.7d}$$

For region II, the solution to the expression were compute by (Hill, 1956). The expression were:

$$\sigma_{rr} = \sigma_{\theta\theta} = \sigma_{zz} = \sigma_m = k\left(1 + \frac{3\pi}{2} - 2\theta\right) \tag{2.8a}$$

$$\sigma_{r\theta} = k \tag{2.8b}$$

For region III the expression were given:

$$\sigma_{rr} = k(1 + \cos 2\theta) \tag{2.9a}$$

$$\sigma_{\theta\theta} = k(1 - \cos 2\theta) \tag{2.9b}$$

$$\sigma_{r\theta} = -k \sin 2\theta \tag{2.9c}$$

$$\sigma_{zz} = \sigma_z = k \tag{2.9d}$$

2.2   3D Crack Tip Field

2.2.1   Elastic-Plastic Stress Fields

(KIKUCHI & YANO, 1990) have done a study related to the HRR stress field at the three-dimensional crack tip. The study was conducted to investigate the effect of thickness on the CT specimen to the stress and displacement field. The research was conducted using 4 type of thickness. the thickness of the specimen is set to be 1 inch, 0.5 inch, 0.25 inch and 1/8 inch. The research is done to see whether the stress field will follow the HRR field when the thickness is changed. The research is started by creating the mesh for the specimen. Meshing of the specimen was shown for only the 0.25 inch specimen. In the meshing the total number of elements is 396 and the number of joints is 2155. In the x-y plane the number of elements is 66 and the number of joints is 235. The specimen is divided in to 6 layer throughout the thickness. the material is taken to be A 533 steel with σ_{fs} of 550 MPa and J_{Ic} of 115.0 kN/m. the experiment then carried out using elastic-plastic FEM analysis until the J value exceed the J_{Ic} value.

For the result if this research shows that the J value for every specimen at the free surface is the largest at the beginning of deformation but when the deformation proceeds the J value at the centre of specimens is relatively decreases. Next is the result of stress field for 1 inch and 1/8 CT specimens. In 1 inch thick specimens, if we compare with HRR solution, the stress field coincides well. From the beginning of deformation until the J value reaches the J_{Ic} value but for the 1/8 inch specimen, the stress field at the beginning of the deformation is coincides well with HRR field but it deviates as the deformation proceeds. For the result of change of stress field along the thickness direction, the stress field on 1 inch and 1/2 inch specimens shows that shows that the plane strain HRR field exists at the centre of specimens. The stress field on the ¼ inch

is smaller if compared to plain strain HRR field and for 1/8 inch specimens, the large difference between result and plain strain HRR field.

The experiment done by (KIKUCHI & YANO, 1990) shows that stress field affected when the thickness of the specimens is changed. The decreases of the thickness will deviated the stress field from the plain strain HRR field. In this paper, it was shown that the HRR field were affected to by the specimens dimensions.

CHAPTER 3

METHODOLOGY

3.1   Introduction

The research was conducted completely using numerical method in which no experimental method involved in this research. The specimen was examined using Finite Element Analysis(FEA) method that was conducted using Abaqus software. The purpose of this section is to describe the method involve in conducting the research. This section consist of a few sub-section, such as modelling, boundary condition determination, material response, specimen meshing and validation. There is two main parts in the analysis in which called pre-processing and post processing. All the sub-topic in the methodology part falls in the pre-processing section. In the modelling section, the specification of the specimen will be explained in details from the type of specimens used in the research until the dimension of the specimens. Boundary condition determination section will explain the details of the load applied to the specimens and the location of the load applied. Material response section explains the property of the material used for this experiment and the calculation of the property influenced of the strain hardening. Meshing section will explains the details on how the mesh were developed on the specimens, the type of the mesh and the element type used for the research. The pre-processing parts were described as in the Figure 3.1.
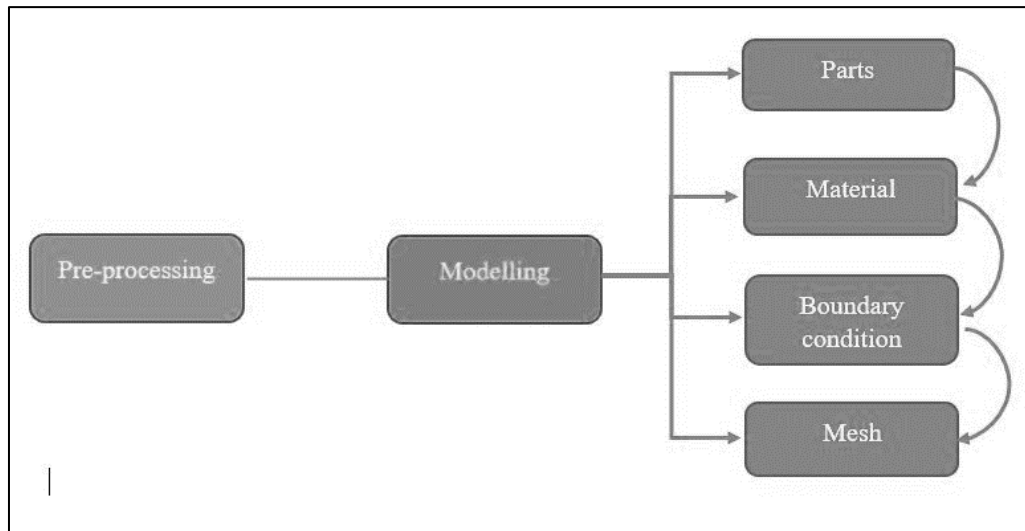
Figure 3.1   Flow of the analysis

3.2   Compact Tension Specimen Modelling

Compact tension(CT) specimen will be used to conduct the analysis in this research. The Compact Tension specimen are consist of sharp crack in the middle and two hole where the load will be applied. A standard Compact Tension have been developed where the standard specification is based on the model of ASTM E399. ASTM E399 was selected because of the model itself were created specially for plain-strain fracture toughness analysis. The full specification is shown in the Figure 3.2.
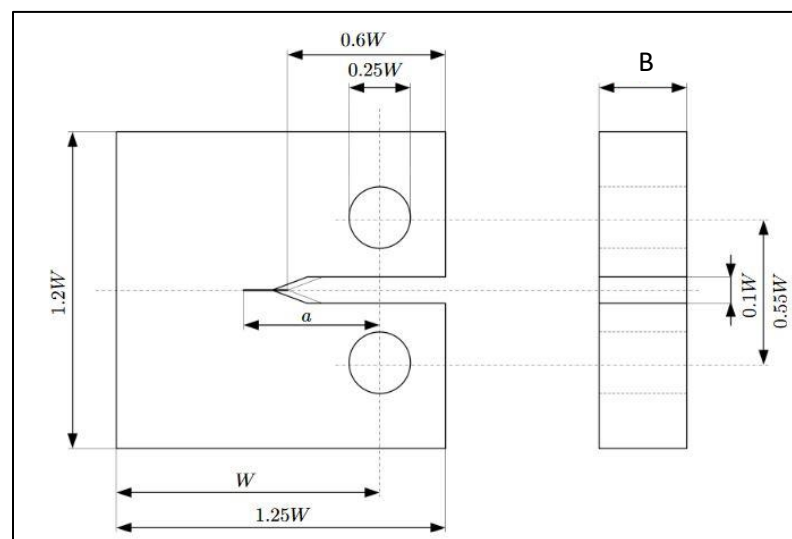
Figure 3.2   Standard Specification of Compact Tension specimen based on ASTM E399

The notation a, W and B represent crack length, width and the specimen thickness. The thickness and width are self-assumption in this research but the value for crack length are obtained from the calculation using formula as below:

$$\frac{B}{W-a} = 1 \qquad (3.1)$$

Because of the research was conducted based on plain strain, the formula must be equal to 1. All the notation in the standard specification are in unit of millimeters(mm). The value for both B and W are assumed to be 16.25 mm and 25 mm and the calculation of the crack length are as below:

$$\frac{25}{12.5-a} = 1 \qquad (3.2)$$

Based on the calculation above, the value of crack length was obtained to be 8.75 mm. All the value obtained then used to developed a full-field Compact Tension specimens. The specimens was developed using Abaqus software. The developed specimen model are shown in the Figure 3.3.
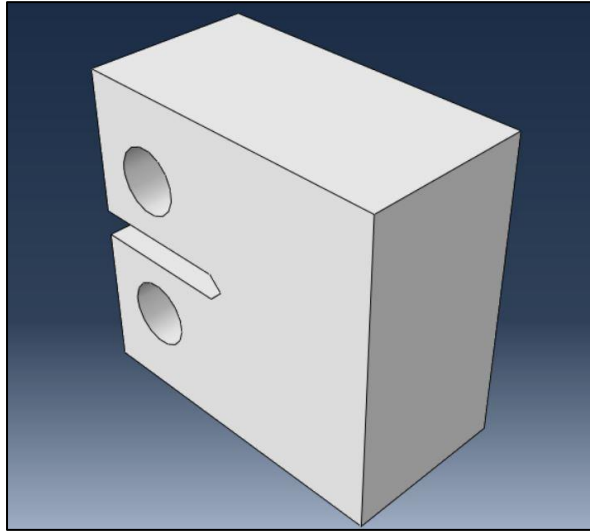
Figure 3.3   Full Field Compact Tension(CT) specimen

Basically the model are symmetrical on both load hole. The model then are reduced to ¼ of the full specimen. The specimen then cut in half in the width and half in the thickness side. Because of the specimen symmetrical, the size of the specimen can be reduced to reduce the time taken to complete the analysis. In mesh development, the symmetrical side will produce same shape of mesh which cause the mesh development and analysis time increase. the finalised model of Compact Tension(CT) specimen are shown in the Figure 3.4.
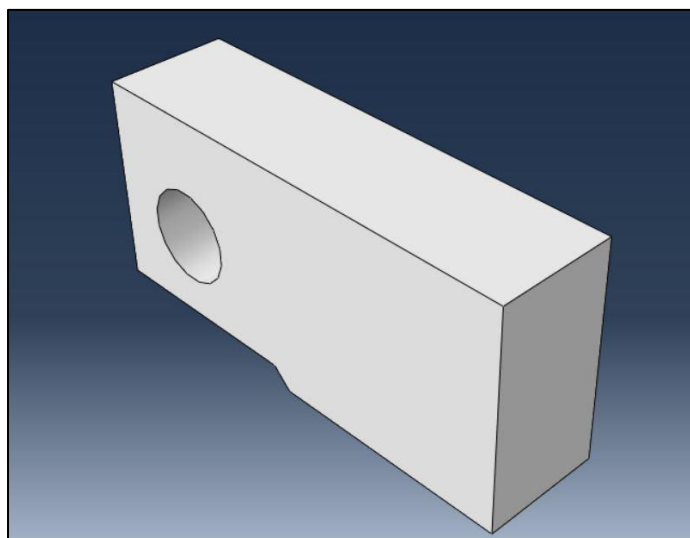
Figure 3.4   Finalised specimen used for Analysis

3.3　Material Properties

The analysis were carried out by using the elastic-perfectly plastic of material properties that is based on uni-axial idealization of the form:

$$\sigma = E\varepsilon; \qquad \sigma \leq \sigma_0; \qquad \sigma = \sigma_0 \qquad \sigma \leq \sigma_o \tag{3.3}$$

Where σ is the uni-axial stress, σ_0 is the yield stress, E is the Young's modulus and ε is the plain strain. The material is assumed to be homogenous isotropic. the analysis were carried out with the material properties of Young's modulus, E = 200 GPa and yield stress, σ_0= 200 MPa. The gain the generality of the result, most of the result were presented in dimensionless form.

An independent analysis were carried out for elastic perfectly-plastic and analysis for strain hardening for the Compact Tension(CT) specimen. For elastic perfectly-plastic analysis, the analysis were carried out based on the boundary condition formulation but for the strain hardening the material response are influenced of the strain hardening effect. The model of strain hardening analysis utilize a power-law hardening model to characterize the uni-axial true stress. The formulation for strain hardening analysis were expressed as below:

$$\frac{\varepsilon}{\varepsilon_o} = \frac{\sigma}{\sigma_o} \qquad \varepsilon \leq \varepsilon_o \; ; \qquad \frac{\varepsilon}{\varepsilon_o} = \left(\frac{\sigma}{\sigma_o}\right)^n \qquad \varepsilon > \varepsilon_o \tag{3.4}$$

Where n is the strain hardening exponent, σ_0 is the yield stress, ε is the plain strain and E is the Young modulus. ε_o is elastic strain limit and the values are obtained through some calculation using the formula. The formula are expressed as below

$$E = \frac{\sigma_o}{\varepsilon_o} \tag{3.5}$$

The analysis were carried out to investigate the strain hardening effect in the material to the stress field formed during the tensile test. The strain hardening in the formula were set to ranges from 1 to infinite number. On strain hardening analysis, the strain hardening exponent were set to be n = 10, 30, 50, 100, and 1000. The ranges in the strain hardening exponent are used to characterize the effect of stress field in the CT specimen when exposed to the strain hardening. The effect of strain hardening were observed in the material at the low strain hardening exponent, n =10 and on the high strain hardening exponent, n = 1000. Elastic strain limit, ε_o in the analysis basically were determine by self-assumption which the values ranges from 0 to infinite number but in the analysis the value of elastic strain limit were set to ranges from 0 to 0.2. Strain, $\varepsilon_o = 0$ indicate the original form of the specimen where specimen are not yet applied to the load and at strain, $\varepsilon_o = 0.2$ indicate the complete form of the CT specimen after load being applied. To increase the accuracy of the analysis, the incrementation of the elastic strain limit which means the smaller the incrementation, the higher accuracy of the analysis. The incrementation for this analysis is set to be 0.005 on every values.

The values obtained then were substituted in the equation to obtain the value of stress. To speed up the calculation process, the equation then were written into the Microsoft Excel for the calculation process. The value of stress then used to plot the relationship of stress and strain. The plot is used to observe the elastic limit of the material in influence of strain hardening exponent. The calculated valued of stress then tabulated in a table and were shown in the Table 3.1

Table 3.1   Stress-Strain relationship at $n = 10, 30, 50, 100, 1000$

Plain Strain	Stress, σ (MPa)				
	n = 10	n = 30	n = 50	n = 100	n = 1000
0	0.00	0.00	0.00	0.00	0.00
0.005	234.92	211.02	206.54	203.24	200.32
0.01	251.79	215.96	209.43	204.66	200.46
0.015	262.20	218.89	211.13	205.49	200.54
0.02	269.86	221.00	212.35	206.08	200.60
0.025	275.95	222.65	213.30	206.54	200.64
0.03	281.02	224.01	214.08	206.92	200.68
0.035	285.39	225.16	214.74	207.24	200.71
0.04	289.23	226.17	215.31	207.52	200.74
0.045	292.65	227.06	215.82	207.76	200.76
0.05	295.75	227.86	216.28	207.98	200.78
0.055	298.58	228.58	216.69	208.18	200.80
0.06	301.19	229.25	217.07	208.36	200.82
0.065	303.61	229.86	217.41	208.53	200.84
0.07	305.87	230.43	217.74	208.68	200.85
0.075	307.99	230.96	218.04	208.82	200.87
0.08	309.98	231.45	218.32	208.96	200.88
0.085	311.87	231.92	218.58	209.09	200.89
0.09	313.66	232.37	218.83	209.21	200.90
0.095	315.36	232.78	219.07	209.32	200.91
0.1	316.98	233.18	219.30	209.43	200.92
0.105	318.53	233.56	219.51	209.53	200.93
0.11	320.01	233.92	219.71	209.63	200.94
0.115	321.44	234.27	219.91	209.72	200.95
0.12	322.81	234.60	220.10	209.81	200.96
0.125	324.13	234.92	220.28	209.89	200.97
0.13	325.41	235.23	220.45	209.98	200.98
0.135	326.64	235.53	220.62	210.06	200.98
0.14	327.83	235.81	220.78	210.13	200.99
0.145	328.98	236.09	220.93	210.21	201.00
0.15	330.10	236.36	221.08	210.28	201.00
0.155	331.18	236.61	221.23	210.35	201.01
0.16	332.23	236.86	221.37	210.41	201.02
0.165	333.26	237.11	221.50	210.48	201.02
0.17	334.25	237.34	221.64	210.54	201.03
0.175	335.22	237.57	221.76	210.60	201.04
0.18	336.17	237.80	221.89	210.66	201.04
0.185	337.09	238.01	222.01	210.72	201.05
0.19	337.99	238.23	222.13	210.77	201.05
0.195	338.87	238.43	222.24	210.83	201.06
0.2	339.73	238.63	222.36	210.88	201.06

The relationship of stress-strain for every strain hardening exponent were plotted.
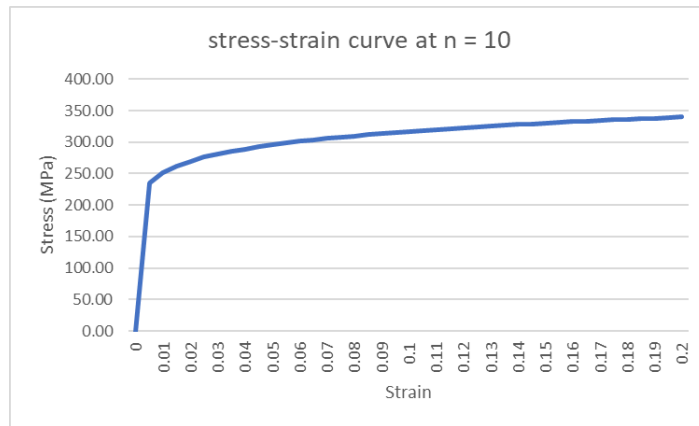
Figure 3.5   Stress-strain curve at n = 10
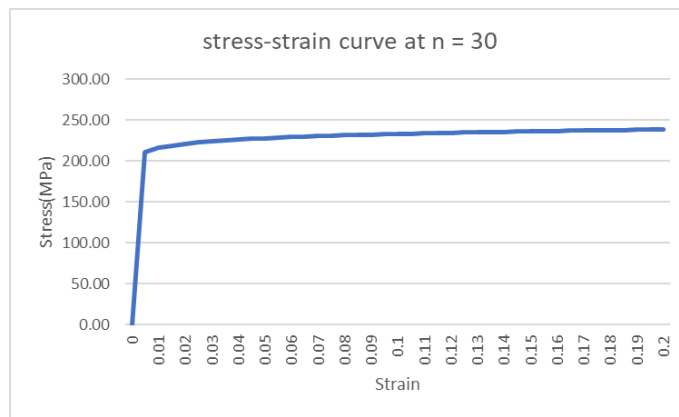
Figure 3.6   Stress-strain curve at n = 30
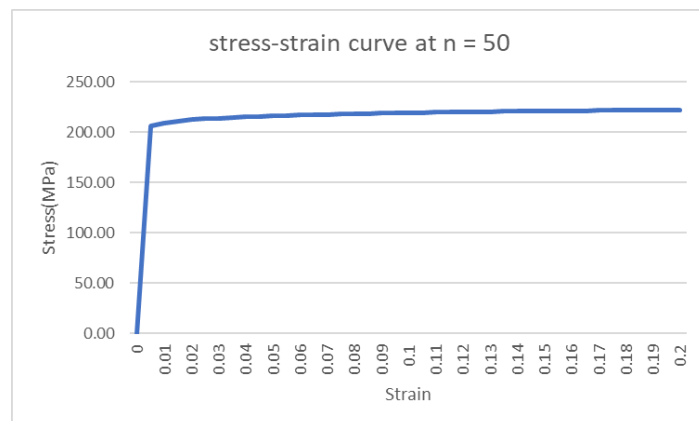
Figure 3.7   Stress-strain curve at n = 50
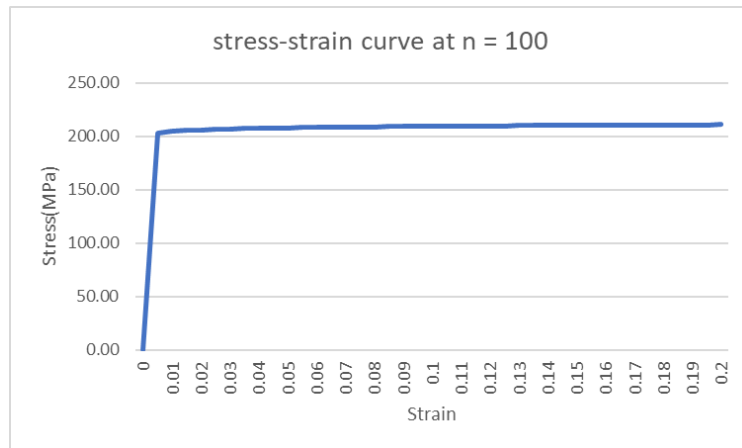
Figure 3.8   Stress-strain curve at n = 100
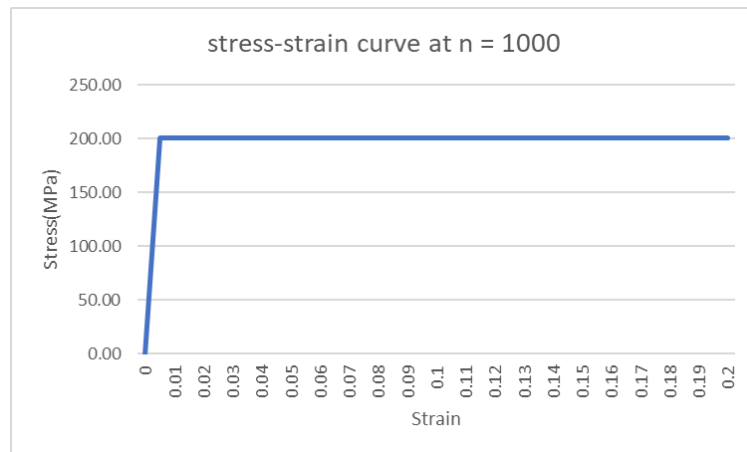
Figure 3.9   Stress-strain curve at n = 1000
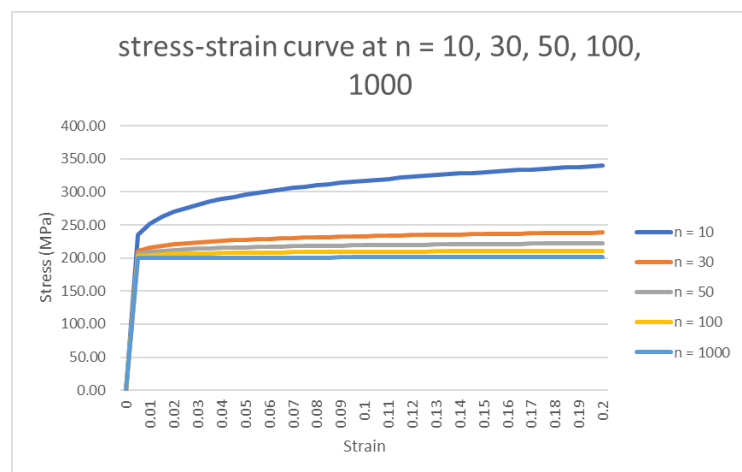
Figure 3.10   Stress-strain curve at n = 10, 30, 50, 100, 1000

3.4   Boundary Condition

This sub-chapter are basically separate in two topic. The first topic will covers up on the load assigning on the specimen where the chapter begin with explaining the loads applied on the specimens the location of the load being applied, and the magnitude of load applied on the specimen. The second chapter is assigning the fixed geometry on the specimen. In this chapter will explain on the importance of the fixed geometry on the specimens and this chapter also explain the location of the assigned fixed geometry.

3.4.1   Assigning the load

The determination of load on the specimen started by determining the load limit of the specimen which called load limit analysis. The load limit analysis is used to determine the tensile displacement of the material in the specimen. This analysis is applying the concept that researched by (Miller, 1988) which provide the limit load calculation geometry that is containing defects. The research provide the load limit, P_o solution for Compact Tension(CT) specimen that is given by:

$$P_o = \frac{2}{\sqrt{3}} W B \sigma_o \left[\sqrt{2.702 + 4.599 \left(\frac{a}{W}\right)^2} - \left(1 + 1.702 \frac{a}{W}\right) \right] \qquad (3.6)$$

For 0.09 < a/W < 1

Where W is the width of the specimen, B is the thickness of the specimen, a is the crack length, and σ_o is the yield stress of the material. The formula created by (Miller, 1988) were used specially for plain strain based problem but the significant of the equation is only limited for a/W from 0.09 until 1. a/w is the ratio of crack length of the specimen divided to the width of the specimen. Basically a/W were determined in the specimen modelling phase. In this research, the a/W ratio used is 0.3 which is within the ranges

of the formula given by (Miller, 1988). The values that used to substitute in the equation are as Table 3.2:

Table 3.2   Values used in the load limit equation

CT width, W	25
CT thickness, B	8.125
Crack length, a	8.75
Yield stress, σ_o	$200 \; x \; 10^6$

The load value then submitted in to Abaqus software. The u_2 displacement caused by plastic limit load is extracted.

The analysis then continued with displacement analysis. the analysis was carried out by applying the displacement, u_2 at the same location of the load limit analysis. The location of load applied is on the loading pin in the specimen. The loading pin location was shown in the Compact Tension Specimen Modelling topics. In this analysis, the loading pin was replace by combination of 9 nodes that is defined as a rigid body in which the rigid body that represents the loading pin. The displacement applied are in direction of y-axis.
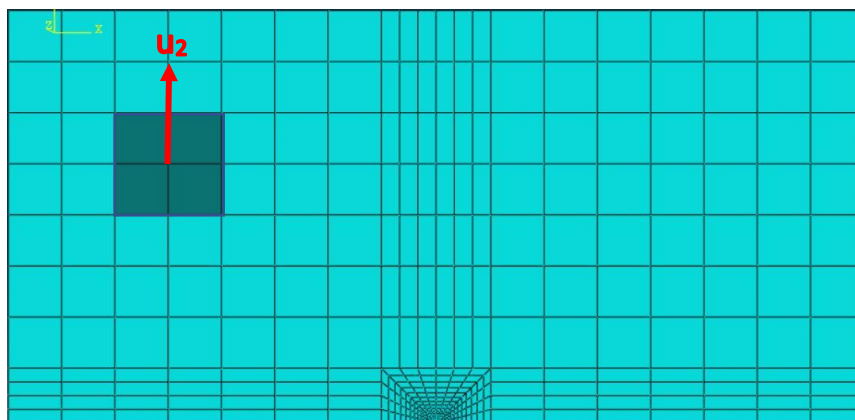
Figure 3.11   Displacement load, u_2 applied on the node that represent loading pin